


Article

Spatial Nonlinear Effects of Street Vitality Constrained by Construction Intensity and Functional Diversity—A Case Study from the Streets of Shenzhen

Jilong Li , Niuniu Kong, Shiping Lin *, Jie Zeng, Yilin Ke and Jiacheng Chen

College of Tropical Agriculture and Forestry, Hainan University, Haikou 570208, China; jllong230@hainanu.edu.cn (J.L.); 22220953000023@hainanu.edu.cn (N.K.); 23210834000007@hainanu.edu.cn (J.Z.); 23210834000003@hainanu.edu.cn (Y.K.); 23220953000012@hainanu.edu.cn (J.C.)

* Correspondence: 990898@hainanu.edu.cn

Abstract: As an important part of urban vitality, street vitality is an external manifestation of street economic prosperity and is affected by the built environment and the surrounding street vitality. However, existing research on the formation mechanism of street vitality focuses only on the built environment itself, ignoring the spatial spillover effect on street vitality. This study uses 5290 street segments in Shenzhen as examples. Utilizing geospatial and other multisource big data, this study creates spatial weight matrices at varying distances based on different living circle ranges. By combining the panel threshold model (PTM) and the spatial panel Durbin model (SPDM), this study constructs a spatial autoregressive threshold model to explore the spatial nonlinear effects of street vitality, considering various spatial weight matrices and thresholds of construction intensity and functional diversity. Our results show the following: (1) Street vitality exhibits significant spatial spillover effects, which gradually weaken as the living circle range expands (Moran indices are 0.178***, 0.160***, and 0.145*** for the 500 m, 1000 m, and 1500 m spatial weight matrices, respectively). (2) Construction intensity has a threshold, which is 0.1466 under spatial matrices of different distances. Functional diversity has two thresholds: 0.6832 and 2.2065 for the 500 m spatial weight matrix, and 0.6832 and 1.4325 for the 1000 m matrices, and 0.6832 and 1.2724 for 1500 m matrices. (3) As an international metropolis, street accessibility in Shenzhen has a significant and strong positive impact on its street vitality. This conclusion provides stakeholders with spatial patterns that influence street vitality, offering a theoretical foundation to further break down barriers to street vitality.

Keywords: street vitality; built environment; threshold effect; spatial effect; spatial autoregression; construction intensity; functional diversity



Citation: Li, J.; Kong, N.; Lin, S.; Zeng, J.; Ke, Y.; Chen, J. Spatial Nonlinear Effects of Street Vitality Constrained by Construction Intensity and Functional Diversity—A Case Study from the Streets of Shenzhen. *ISPRS Int. J. Geo-Inf.* **2024**, *13*, 238. <https://doi.org/10.3390/ijgi13070238>

Academic Editors: Wolfgang Kainz, Raja Sengupta, Shivanand Balram and Jorge Rocha

Received: 9 May 2024

Revised: 28 June 2024

Accepted: 30 June 2024

Published: 2 July 2024



Copyright: © 2024 by the authors. Licensee MDPI, Basel, Switzerland. This article is an open access article distributed under the terms and conditions of the Creative Commons Attribution (CC BY) license (<https://creativecommons.org/licenses/by/4.0/>).

1. Introduction

Streets and the vitality of cities are strongly related and as observed by Jane Jacobs “if the streets are vibrant, the city is also Vibrant” [1]. Streets, as the basic units of urban life, not only serve the function of city transportation, but are also important venues for residents’ activities and are a concentration of urban vitality [2]. People use streets for socializing, leisure, and other functional activities; thus, streets are increasingly seen as social spaces rather than merely spaces for mobility [3]. Prosperous, bustling streets can enhance human activity and social interaction, facilitate transactions, and attract talent and capital, thereby boosting urban competitiveness and creativity, maintaining urban resilience, and ultimately achieving sustainable development [4]. Jacobs first identified four formative conditions for street vitality: mixed-use, density, new and old buildings, and short streets, which spurred exploration into the mechanisms of street vitality formation [2,5]. In recent years, the rapid development of information technology and the use of multisource big data have led people to re-examine and verify street vitality. Street vitality is considered a complex

concept occurring in urban street spaces, closely related to the built environment itself and having distinct spatial characteristics [6–10].

Due to the proximity effect, elements in geographic space often impact their surroundings, a phenomenon typically manifested as spatial effects [11–15]. Street vitality is clearly influenced by other streets within a certain range; when a street's vitality changes due to positive or negative factors, this change acts as either positive or negative feedback on the surrounding streets [16]. However, previous studies based on geographic big data were limited to exploring the impact mechanisms of the streets' own built environment on street vitality, considering the built environments of streets as independent and not accounting for spatial or group dependencies [17], thus overlooking the important role of spatial effects in the formation of street vitality. Although the existence of regional interactions has been confirmed, the spatial scale and range of these spatial effects remain unknown, particularly when streets are used as the basic research unit; how the distance decay mechanism of spatial effects manifests is still unknown [18]. Clarifying the spatial effects of street vitality at different geographical distances helps to quantitatively describe this influence mechanism. While most scholars focus on analyzing the interrelationship between street-built environments and street vitality, they often overlook the exploration of urban vitality's spatial effects, with the built environment acting as a constraining factor [19,20]. Wu and others' research method accounts for both spatial and nonlinear effects, but it primarily focuses on urban vitality by dividing Shanghai into 72 research units [21]. Our study concentrates on the linear aspects of street spaces, which are smaller in scale and have a larger sample size, thus providing a micro-level supplement to their work.

Methods, such as least squares regression, multiple linear regression, geographically weighted regression, and the entropy weight model, have provided various effective approaches for exploring the formation of street vitality [22–24]. However, these methods assume a potential linear relationship, which may overestimate or underestimate the nonlinear effects of variables. Moreover, when using these methods, it is challenging to integrate the nonlinear effects and spatial effects of street vitality. Recently, Han et al. observed that the relationship between certain urban morphological characteristics and street vitality is nonlinear, with correlations changing dramatically upon exceeding specific thresholds of these attributes [25]; meanwhile, with the widespread use of machine learning, Xu et al. employed the random forest method to reveal the nonlinear effects of street features on pedestrian perception, and Li et al. identified street vitality automatically through deep learning based on the number of pedestrians and the classification of activities on the streets, and used street view semantic segmentation to measure five selected street building environment variables related to vitality, providing us with a new perspective for further understanding of the built environment [26,27]. Additionally, Zhao et al. systematically analyzed the spatiotemporal heterogeneity of the built environment's impact on street vitality by constructing a geographically and temporally weighted regression (GTWR) model, providing insights into exploring nonlinear and spatial effects [28]. Based on this, we constructed a model that can describe nonlinear (particularly in pursuit of thresholds) and spatial effects, namely the spatial autoregressive threshold model. This model analyzes the spatial nonlinear effects of neighboring streets on the vitality of a given street under different built environment constraints.

Over the past few decades, the rise of the Internet has made the acquisition of multi-source geographic big data possible, providing a new avenue for quantitative research into the mechanisms of street vitality formation. Many scholars have begun to use data, such as POIs, public reviews, social media check-ins, location tracking, and mobile signaling [29–33], employing projection pursuit models to analyze urban vitality from multiple perspectives and dimensions, including fuzzy comprehensive evaluation and spatial analysis, achieving significant progress. The increasing prevalence and use of location-aware technologies enable people to add location data to online social networks in various ways, such as by posting reviews at event locations (like public reviews) or leaving notes at specific places (e.g., Gaode Maps, Baidu Maps). The widespread use of location-based

services (LBS) has provided researchers with unprecedented opportunities to mine and visualize location-based tracking data and social media data, enhancing our understanding of human mobility [34]. Based on this principle, by acquiring urban street geographic information big data, we can conduct extensive macro and micro analyses.

This study aims to investigate the spatial nonlinear effects of street vitality within the constraints of two key indicators of the street built environment. By leveraging multisource big data and integrating the PTM and STDM models, we built a spatial autoregressive threshold model to answer three questions: (1) When street construction intensity and functional diversity fall within different threshold ranges, are the effects of threshold variables and their control variables on street vitality consistent? (2) Do the spatial effects of street vitality adhere to a distance decay mechanism within different living circle distances? (3) When considering spatial effects, is it possible to improve the explanatory power of the street vitality formation mechanism?

2. Literature Review

2.1. Definition and Measurement of Streets and Street Vitality

According to “*Cihai*”, a street is defined as “a relatively wide urban road flanked by buildings, typically referring to road sections that have shops facing the street” [34]. From this, it can be deduced that the most important characteristic of a street is to provide a public space for social interaction and transactions; streets are not entirely synonymous with urban roads, which prioritize fast traffic, while streets emphasize slower traffic and spaces for social activities.

Streets, as the public spaces most characteristic of urban areas, are rarely mentioned in the normative documents of our country’s planning and design system and are often represented as “urban roads”. Therefore, urban planning standards merely continue the method of traffic categorization, lacking a category for “urban street planning” and primarily focusing on “urban road system planning”. According to the 2012 revised *Urban Road Engineering Design Specifications*, urban roads are classified into expressways, arterial roads, secondary arterial roads, and branch roads; since expressways primarily serve a transit function, they are not within the scope of this study [35]. The streets mentioned in this article are those where the urban main arteries, secondary arteries, and branch roads extend from the centerline to a certain distance on both sides, including all buildings and their setback spaces on both sides containing POIs.

Jane Jacobs noted that urban streets act as lines on a macro level and as surfaces on a micro level, which are crucial in forming public activity spaces within cities. She observed that while these spaces serve as venues for public interaction, it is ultimately the people who infuse these spaces with vitality [1]. Jan Gehl, in his book *Life Between Buildings*, stated that vitality comes from human interaction, meaning that the vitality of street public space is generated by human activities. He emphasized that slow traffic can promote street vitality [36]. In 1998, Montgomery characterized “street vitality” as encompassing pedestrian flow, the utilization of facilities, and the prevalence of cultural activities along streets [37]. In summary, people and their activities are the foundation of street vitality. The physical environment of streets provides a place for activities and influences people’s behavior [38].

With the popularization and widespread application of big data, real-time pedestrian flow data on streets has become more accessible, and researchers often use the intensity of a street’s active population to represent it. Spatial big data containing geographic location information, such as Baidu LBS data, Baidu Heatmap data, and mobile signaling data, are frequently used to measure street vitality. For instance, Han, Patrizia, and others used social network review data and location data to represent street vitality [17,39,40]. Xia, Kim, and others used mobile location information to represent street vitality [41–43]. Zeng, Liu, and others used traffic trajectory data to represent street vitality [44–46].

2.2. *The Role of the Street Built Environment in the Mechanism of Street Vitality Formation*

Various factors of the built street environment impact street vitality. Bernick and Cervero characterized the built environment from three dimensions: density, diversity, and design [47]. Later, Belzer and Autler added two more dimensions, namely transportation distance and destination accessibility, to evaluate the built environment [7,48]. Jacobs emphasized the importance of street diversity and construction intensity (density) for street vitality. In his 1998 study, Montgomery underscored “development intensity” as a critical driving force behind vibrant urban life [49]. Based on an empirical study of Chengdu’s street space, Li and others found that construction intensity has the greatest impact on street vitality within a certain scale [50]. Wu and others’ research shows that functional diversity plays a significant role in enhancing street vitality [7]. However, some studies have found that construction intensity can have entirely different effects at different stages of urban development [51]. Wu and others found that when streets have varying levels of construction intensity, increasing functional diversity also produces different impacts [32]. Construction intensity and functional diversity have spatial clustering and spillover effects. Different streets have different spatial geographic positions, so the mechanisms by which construction intensity and functional diversity impact street vitality need further exploration.

2.3. *The Impact of Spatial Effects on Street Vitality*

In 1933, German geographer Walter Christaller introduced the central place theory, which describes how town centers serve surrounding areas, and laid an early theoretical groundwork for understanding spatial effects [52]. Subsequently, Swedish economic geographer Tord Palander emphasized the role of spatial factors in enhancing economic vitality. Fu and colleagues examined the spatial spillover effect in urban clusters and discovered that this effect is not a simple linear relationship. Instead, as distance increases, it first strengthens and then weakens in an inverted U-shape [53]. Xiang and others showed that infrastructure in neighboring areas has a positive effect on local economic growth, demonstrating the positive spillover effects of infrastructure development within the Shenyang economic region [54]. Hu and others, based on the characterization of POI data, studied the spatial agglomeration and boundary effects in Ningbo, revealing significant clustering patterns in commercial spaces [55]. Although previous research has begun to focus on the spatial effects of built environment factors, such as infrastructure and commercial activities on urban vitality, most of this research is on a large scale and lacks street-level studies to explore the thresholds and boundaries of spatial effects.

3. Scope of Research and Data

3.1. *Research Scope*

Located in southern Guangdong Province, Shenzhen is a coastal city on the eastern shore of the Pearl River Estuary, directly adjacent to Hong Kong. It is bordered by Daya Bay and Dapeng Bay to the east, the Pearl River Estuary and Lingding Yang to the west, and is connected to Hong Kong by the Shenzhen River to the south. To the north, it neighbors are the cities of Dongguan and Huizhou. Shenzhen is located south of the Tropic of Cancer, between longitude 113°43′ and 114°38′ east, and latitude 22°24′ and 22°52′ north. The total area of the city is 1997.47 square kilometers. In 2023, Shenzhen’s GDP reached CNY 3.46 trillion, ranking third in the nation after Beijing and Shanghai. The registered total population of Shenzhen’s communities in 2023 was 21.6377 million, making it a major first-tier city in China. Based on these economic and demographic factors, Shenzhen’s vitality has been enhanced. By selecting Shenzhen as the research area to examine the spatial nonlinear effects of street vitality at different thresholds of street construction intensity and functional diversity, this study can offer robust suggestions for future development and stimulating street vitality in new first-tier, second-tier, and third-tier cities in China, as well as in cities of developing countries.

As shown in Figure 1, this study takes the street spaces of Shenzhen as the research object. Referring to the *Code for Urban Road Engineering Design* and the OSM open road network's road classification standards, and considering the setting of buffer zones for calculating street-related indicators, this paper classifies streets with an interface width (including certain spaces, like plazas formed by building setbacks on both sides of the street) of 140 m or more as main roads, those between 90 and 140 m as secondary roads, and those between 50 and 90 m as branch roads. Finally, based on factors, such as road intersections and rivers, the streets are divided into several segments, resulting in a total of 5290 street samples. Considering that Jan Gehl emphasized that slow traffic is an important condition for fostering street vitality, this paper divides the street into three parts on the plan: the first is the vehicular lane, the second is the sidewalks on both sides of the vehicular lane, and the third is the setback space between the vehicular lane and building facades. In calculating street pedestrian flow, the vehicular lane part is excluded, and only the vitality values of the remaining two parts are calculated [35].

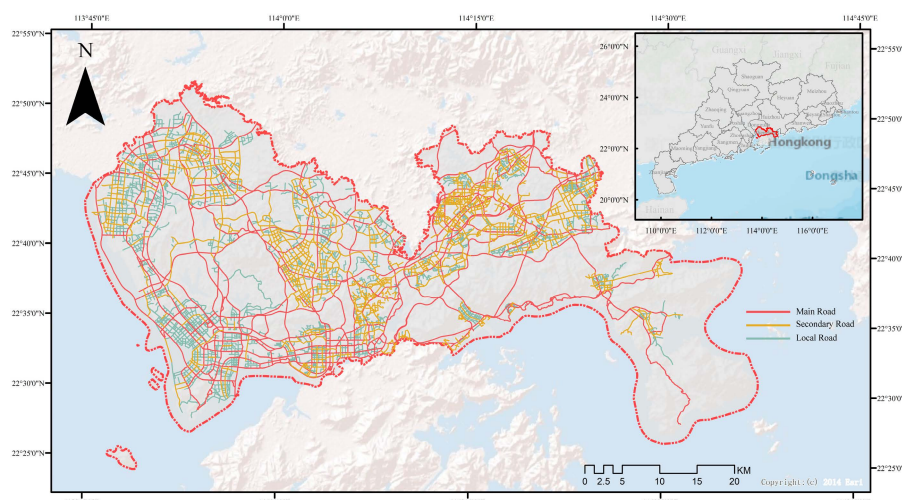


Figure 1. Research scope and road network data.

3.2. Data Collection and Cleaning

We have obtained road network data, Baidu Huiyan LBS data, Amap POI data, and Baidu building data. The data statistics are as shown in Table 1.

Table 1. Summary of basic data.

Data Type	Source	Description	Link
Baidu building data	a	Contains 663,184 records	" https://map.baidu.com/ (accessed on 14 June 2022)"
Baidu Huiyan data	b	Total of 5290 segments	" https://huiyan.baidu.com/ (accessed on 15 June 2022)"
Amap POI data	c	Total of 3,506,483 records	" https://ditu.amap.com/ (accessed on 14 July 2023)"
Road network data	d	Total of 761,414 records	" https://www.openstreetmap.org/ (accessed on 24 October 2023)"
Street view images	a	A total of 158,612 valid street view images	" https://map.baidu.com/ (accessed on 7 June 2024)"

Note: a: Baidu Maps; b: Open Street Map official website; c: Baidu Huiyan; d: Gaode Maps Open Platform.

3.2.1. Road Network Data

Based on the road network downloaded from OSM and satellite map data from Baidu Maps, we manipulated the data using ArcGIS Pro 3.0.0 to split and extend it as required by the study, to obtain complete and accurate centerline data for streets. We ultimately obtained 882 arterial roads, 1861 secondary roads, and 2547 minor roads, totaling 5290 segments.

3.2.2. Baidu Huiyan LBS Data

We obtained Baidu Huiyan population grid data for a continuous week from 10 July to 16 July 2022, amounting to 168 time points of LBS data. Compared to the data from April, the second quarter, the vitality of Shenzhen's streets was higher in July, hence we selected data from this week in July as our sample base. The original data does not show specific population distributions at any given time point but is based on a grid system, recording the frequency of calls to the Baidu SDK within a 200 m grid every hour, representing a relatively coarse set of data. To better represent this specific population distribution, we used the Random Points tool in ArcGIS Pro to simulate and generate street population distributions. For streets of different classifications, we used different ranges of spatial connections to derive the relative population numbers within the street's extent. To eliminate errors caused by unusual conditions at any specific time point, we used the mean of the relative population numbers from 168 time points over the week as the relative population number for that street.

3.2.3. Amap POI Data

As China's digitalized cities continue to develop, urban spatial carriers are abstracted into points of interest and presented to users through map apps. The Amap Open Platform provides various functions for querying POI information. In this study, we searched Shenzhen using POI categories (data collected in September 2023), obtaining 19 major categories totaling 761,414 valid entries.

3.2.4. Baidu Building Data

Using Python-based web scraping technology, we obtained building data for Shenzhen for the years 2019 and 2023 (including certain fields, such as the number of building floors, and land area). Due to partial data loss in 2023 (suburban areas missing), we combined data from 2019 and 2023 and cleaned it to obtain a more complete set of building outline data for Shenzhen, totaling 663,184 records.

3.2.5. Street View Images

Simultaneously, based on the road network data of the study, street view sampling points were generated every 100 m along the road network. For roads shorter than 100 m, sampling points were generated based on the road endpoints. Finally, street view images were obtained using Python, resulting in a total of 158,612 valid street view images. The following Figure 2 shows the semantic segmentation results of the street view image at point number 164 on a secondary road: the sky represents 19.5% of the image, grass is 2.9%, and trees are 6.9%.

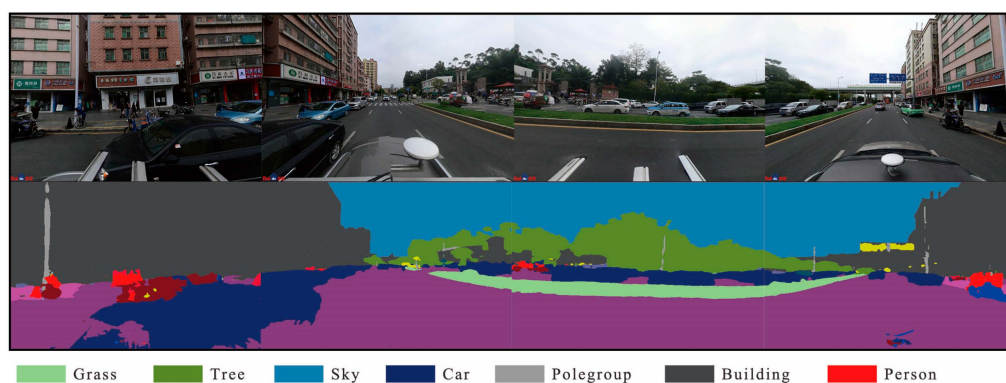


Figure 2. Semantic segmentation results of street view.

4. Methodology

4.1. Explanatory Variables

Streets, as one of the largest public spaces in cities, carry profound social and cultural implications [37]. Within the context of urban geography and urban planning, street vitality is widely classified as the enduring force of urban streets [56], the diversity of urban life [1], or the activities of people on the streets [36]. To maintain street vitality, an active population density must reach a sufficiently high level to facilitate interaction between people and space, leading to transactions and social interactions. With the rapid development of the Internet, the use of mobile phones for socializing, navigation, payments, etc., has become extremely common among urban residents. These mobile Internet services record users' locations, generating passive LBS data, which, after being anonymized and aggregated, can be used for urban big data analysis. Therefore, this study uses a week's worth of continuous LBS data to quantify street vitality (Table 2), with the following calculation method:

$$\bar{H} = \frac{1}{7 * 24} \sum_{i=1}^7 \sum_{j=1}^{24} P_{ij} \quad (1)$$

where \bar{H} represents the average heat value of a street over a week, i represents the i -th day of the week ($i = 1, 2, \dots, 7$), j represents the j time point of a day ($j = 1, 2, \dots, 24$), and P_{ij} represents the relative population number at a certain time point on a street. The final result will be the linear density (number of people per hundred meters) of the average relative population over seven consecutive days within each street segment, serving as the data representing street vitality.

Table 2. Daily street vitality data statistics.

Date	Relative Population on Streets	Mean	Maximum	Minimum	Standard Deviation
Monday	7,283,132	8.43	550.57	0	12.58
Tuesday	7,209,726	8.37	500.76	0	12.15
Wednesday	7,249,843	8.41	522.80	0.014	12.36
Thursday	7,190,898	8.31	459.81	0.014	11.04
Friday	7,409,353	8.58	566.89	0.011	12.93
Saturday	7,322,311	8.45	485.01	0.022	12.22
Sunday	6,993,683	8.12	522.80	0.017	11.50

Note: mean represents the average relative population per 100 m of street (number of people per 100 m of street).

Based on the above calculation method, the average vitality at specific times between 10 July and 16 for the Shenzhen street units was obtained through visual analysis, as shown in Figure 3:

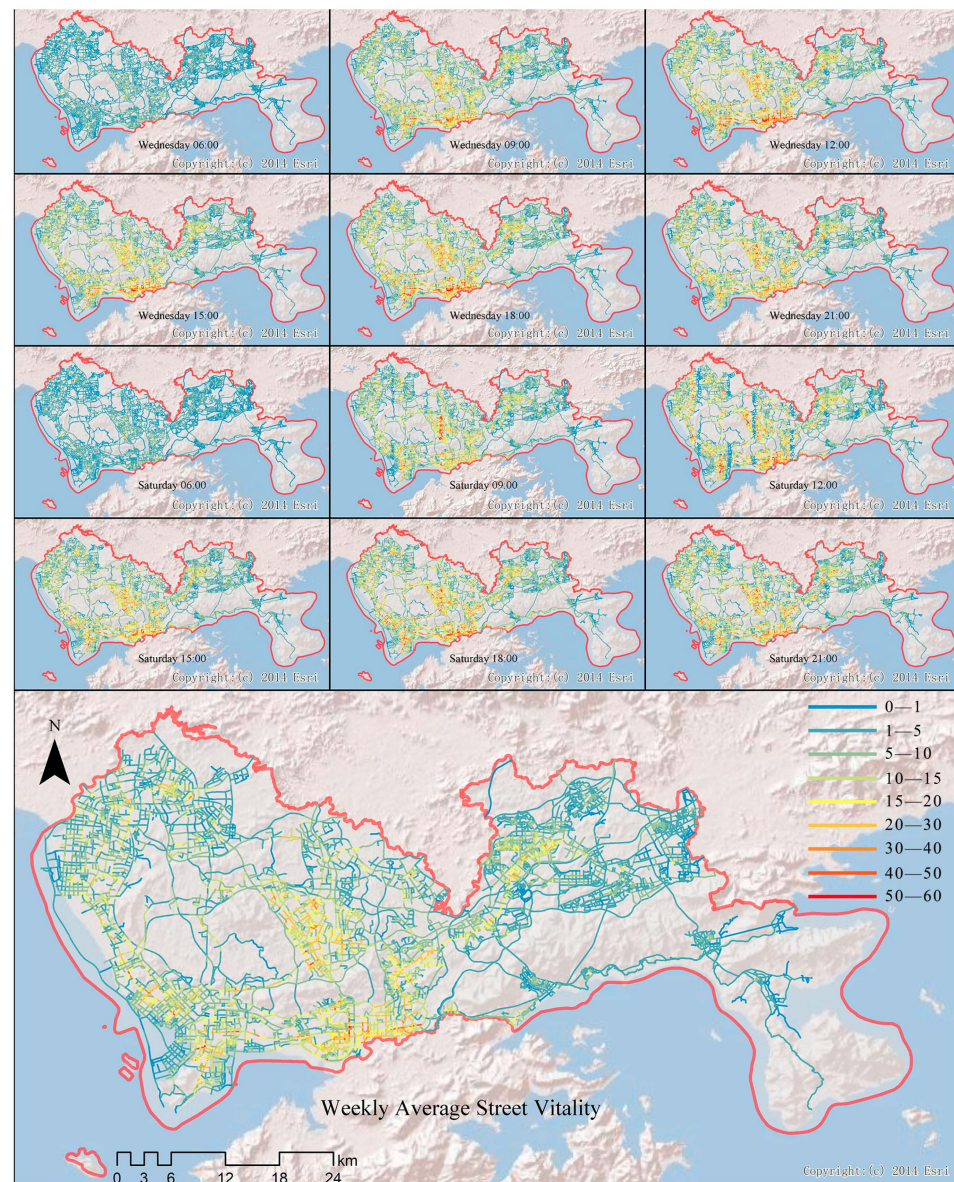


Figure 3. Vitality kernel density map of streets at different time points.

4.2. Threshold Variables and Control Variables

As key metrics of the built environment, construction intensity and functional diversity are utilized as threshold variables in this research [57,58]. Additionally, to more precisely explain the connection between construction intensity, functional diversity, and street vitality, and to improve the interpretability of the model, this article draws on the research of Ma, Wang, and Chen using certain variables, such as accessibility, public service facilities, building footprint density, sky view factor (SVF), and green view index (GVI), as controls [59–61]. The definitions and calculation methods for the threshold variables and control variables are shown in Table 3.

Table 3. Threshold variables and control variables.

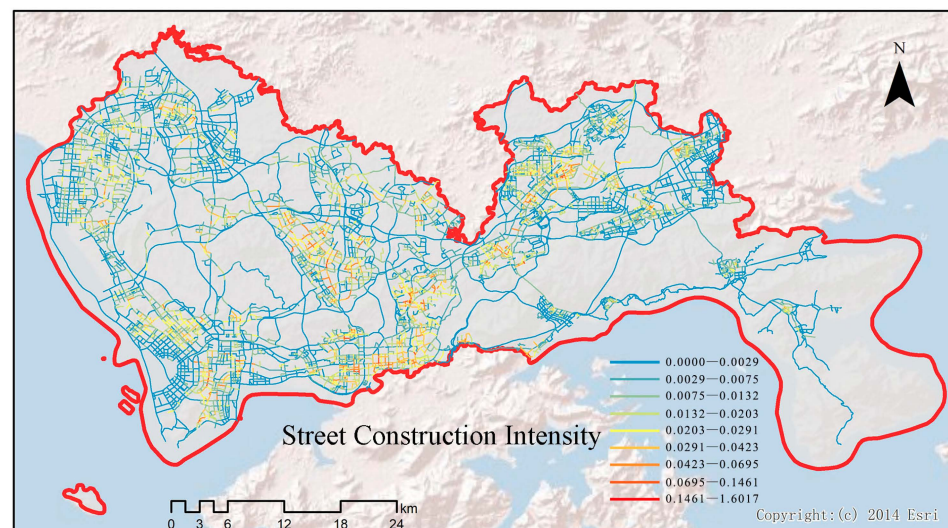
Type	Variable Name	Description
Threshold variable	Construction intensity	Based on street POI data, the linear density of POIs along the streets is used as an indicator of street construction intensity.
	Functional diversity	POIs are categorized into 16 major classes, and the Shannon diversity index is calculated to determine functional diversity.
Control variable	Integration	Standardized angular integration measured using Depthmap.
	Public transport facilities and services	Calculated based on the line density of public transport stations, such as bus and subway stations.
	Public facilities and services	The service level of public facilities is represented by the linear density of three categories of POIs: public amenities, transportation facilities, and government and other social organizations.
	Building occupation density	The total area occupied by buildings on both sides of a certain street divided by the length of the street (square meters per kilometer).
	Sky view factor	The ratio of sky pixels to the total pixel count in street view images.
	Green view index	The ratio of the total pixels of grass and trees to the total pixel count in street view images.

4.2.1. Construction Intensity

This paper characterizes construction intensity by the linear density of the number of POIs within a street area. Depending on the width of arterial roads, secondary roads, and alleys, different distances are used for spatial connections when counting the number of POIs within a street. The specific formula for calculation is as follows:

$$C = \frac{\sum_{i=1}^n N_i}{L} \quad (2)$$

where C represents the construction intensity, n is the number of POI categories, N_i represents the number of the i -th type of POI on the street, and L represents the length of the street. Figure 4 shows the density map of the street construction intensity.

**Figure 4.** Kernel density map of street construction intensity.

4.2.2. Functional Diversity

The article assesses the diversity of functional facilities on streets by using the POI diversity index. Based on the Amap POI classification coding table, researchers catego-

rized the POIs of Shenzhen's streets into 16 main types, including catering services, road ancillary facilities, scenic spots, government agencies, and social organizations, as well as accommodation services. Utilizing the Shannon diversity index, the research team defined the specific formula for calculating the POI diversity index as follows:

$$e = -\sum_{j=1}^n (P_j * \ln P_j) \quad (3)$$

$$P_j = \frac{N_j}{\sum_{j=1}^n N_j} \quad (4)$$

where e represents the diversity of street functions, P_j represents the proportion of the j -th category of POIs, n represents the number of POI categories, and N_j represents the quantity of the j -th category of POIs on a particular street. To account for the absolute number differences between different categories of POIs, we first normalize the number of POIs before calculating their diversity index. Figure 5 shows the map of street function diversity.

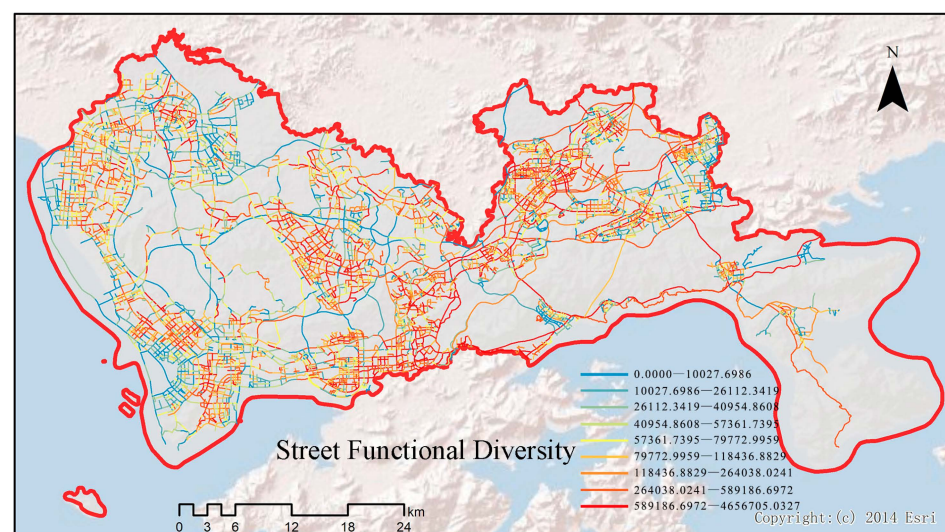


Figure 5. Kernel density map of street functional diversity.

4.2.3. Accessibility

Accessibility ensures that citizens can easily and efficiently reach these activity centers, which promotes social interaction and economic activities on urban streets. We have chosen two indicators to characterize street accessibility: integration and public transportation facilities services.

Integration is a measure of the connectivity of a street to other streets; the higher the integration of a street, the more convenient it is to travel from this street to others, and the better the overall connectivity. We have calculated the integration of streets based on Depthmap, and the formula is as follows:

$$NAIN = (node_count^{1.2}) / (total_depth + 2) \quad (5)$$

where $NAIN$ represents the normalized integration, $node_count$ indicates the number of segments within the global scope, and $total_depth$ represents the total topological depth within the global scope. Figure 6 shows the visualization of the street integration.

Public transportation facilities and services are used to measure the availability and convenience of public transportation. Streets with higher levels of public transportation facility services provide greater convenience for residents relying on public transit, thereby effectively reducing dependence on private vehicles, promoting the development of sustain-

able transportation, and also aiding in the revival of slow traffic, enhancing the functional role of the street as a “street”. Equation (6) is as follows:

$$PTS = \frac{N}{L} \tag{6}$$

where *PTS* represents the density of public transportation facilities and services on the street, *N* is the number of public transit stops, such as bus stations and subway stations within the street area, and *L* represents the length of the street. Figure 7 shows the visualization of the density of public transportation facilities and services on the street.

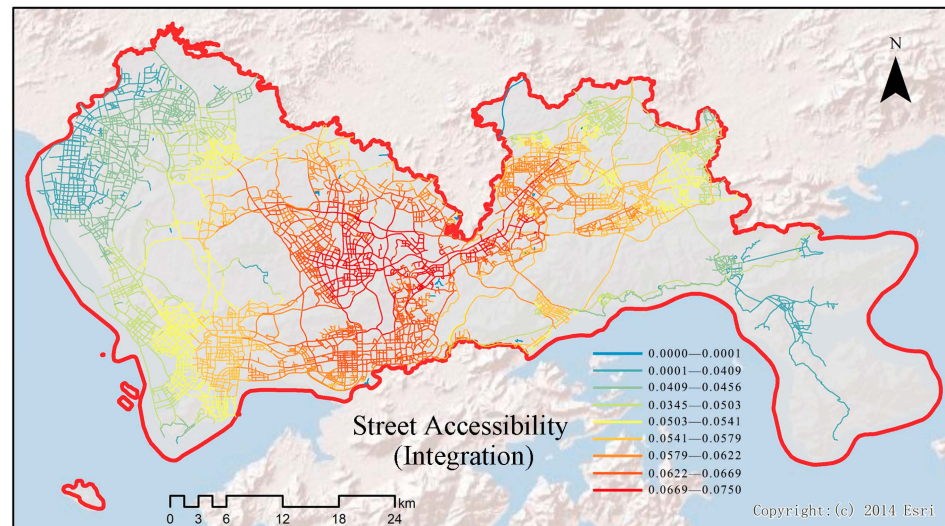


Figure 6. Kernel density map of street integration.

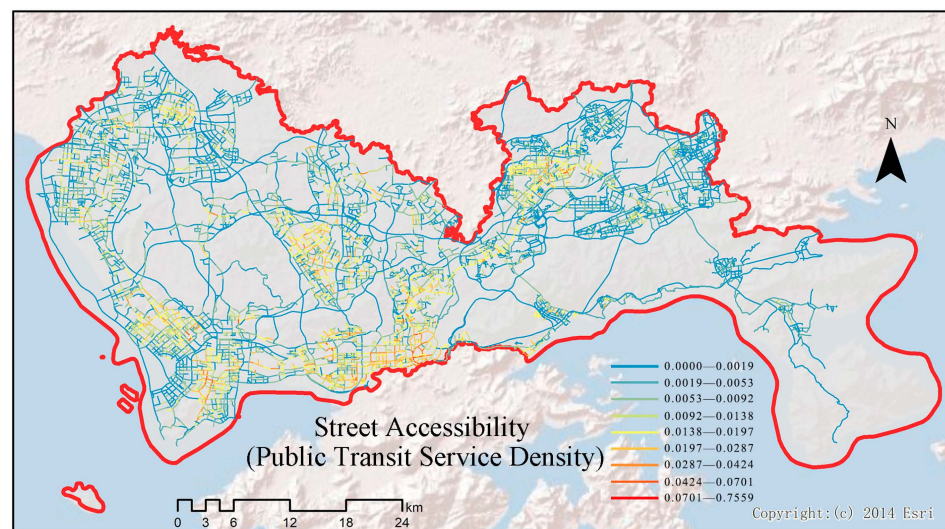


Figure 7. Kernel density map of street public transportation facilities and services.

4.2.4. Public Facilities and Services

This paper uses the linear density of three types of points of interest (POIs)—public facilities, transportation facilities services, and government institutions and other social organizations—to represent public utility services. This approach comprehensively reflects the density of facilities and services available for public use within an area. The calculation method is as follows:

$$PFS = \frac{\sum(N_1 + N_2 + N_3)}{L} \tag{7}$$

where *PFS* represents the density of public facilities and services on the street, indicating the number of POIs for public facilities, transportation facilities and services, and government institutions and other social organizations within the street area. The visualization of this is shown in Figure 8:

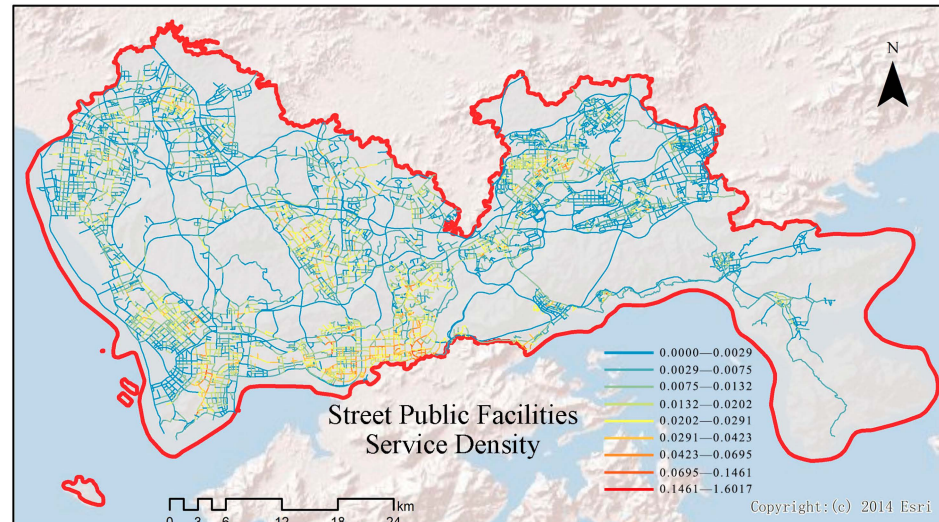


Figure 8. Kernel density map of street public facilities and services.

4.2.5. Building Coverage Density

The building coverage density on streets differs from POI linear density, as it focuses on the actual land use within the street area, including residential, commercial, industrial, and other types of buildings. It reflects the intensity of land use in street spaces. The calculation formula is as follows:

$$b = \sum_{i=1}^n B_i / L \tag{8}$$

where *b* represents the building coverage density, *B_i* represents the footprint area of the *i*-th type of building within the street area, *n* represents the number of building categories, and *L* represents the length of the street. Figure 9 shows the map of building coverage density on the street.

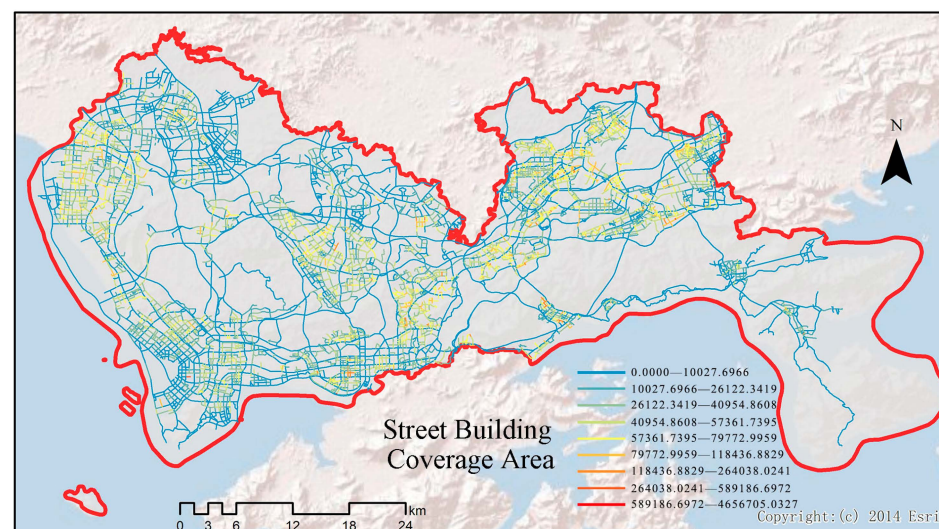


Figure 9. Kernel density map of the street building coverage area.

4.2.6. Sky View Factor

Using street view images, the images are segmented into 19 categories via a deep learning model, and the proportion of sky elements is extracted as needed. The calculation formula is as follows:

$$SVF = \sum_{i=1}^n Sky_i / Total_i \quad (9)$$

where n denotes the number of points within a street segment that include street view images, Sky indicates the pixel size of the sky element, and $Total$ represents the pixel size of the entire street view image.

4.2.7. Green View Index

Similar to the sky view actor, we extract the grass and tree categories from the street view segmentation as elements for calculating the green view index. The calculation formula is as follows:

$$Gvi = \sum_{i=1}^n (Grass_i + Tree_i) / Total_i \quad (10)$$

where n denotes the number of points within a street segment that include street view images, $Grass$ indicates the pixel size of the grass element, $Tree$ indicates the pixel size of the tree element, and $Total$ represents the pixel size of the entire street view image.

4.3. Selection of Distance for Spatial Weight Matrices

The concept of “living circles” originates from Japan, where residents center activities, such as shopping, leisure, social interaction, and healthcare, around their homes, creating spatial or activity spaces [62]. Following the “15-min city” proposed by French scholar Carlos Moreno, numerous scholars have defined concepts, like the 5-min, 10-min, and 15-min living circles, by the distances people can travel slowly (including walking and cycling) within 5, 10, or 15 min [63–66]. Research by Paul et al. found that the average walking speed at uncontrolled crossing points is 1.433 m per second [67]. Studies by Zhang Huiling and others have found that the walking speed of adults is 1.21 m/s, with a stride of 0.69 m and a cadence of 1.80 steps/s [68].

This paper introduces the concept of living circles, defining the influence range of streets as 5-min, 10-min, and 15-min street living circles, and constructing three different geographical spatial weight matrices at distances of 500 m, 1000 m, and 1500 m, respectively. In the spatial weight matrices at 500, 1000, and 1500 m, there are, respectively, 303, 33, and 13 isolates. Taking the 500 m spatial weight matrix as an example, if the distance between the centers of two streets exceeds 500 m, they are considered unconnected with a weight of 0; otherwise, they are considered connected, with the weight being the reciprocal of the distance. Their spatial connectivity is shown in Figure 10.

Using spatial weight matrices at three different distances, the global autocorrelation was tested using Moran’s I index. The results indicate a strong positive spatial autocorrelation in street vitality. Table 4 shows that the Moran’s I index values at distance thresholds of 500 m, 1000 m, and 1500 m are 0.18, 0.16, and 0.15, respectively, all indicating statistically significant spatial clustering patterns (p -value = 0.001).

Table 4. Moran’s I values for different distance weight matrices.

Distance Weight	Moran’s I	p -Value	Standard Deviation	Number of Isolated Islands	Maximum Number of Connections	Average Number of Connections
500 m	0.178	0.002 (12.473)	0.014	303	21	5.029
1000 m	0.160	0.001 (31.014)	0.005	33	54	17.538
1500 m	0.145	0.001 (39.055)	0.004	13	81	35.752

Most data points in the Moran scatterplot (Figure 11) are concentrated in the first and third quadrants, indicating that areas of higher vitality tend to be adjacent to other

high-vitality areas, while low-vitality areas are adjacent to other low-vitality areas. As the distance threshold increases, Moran’s I index decreases, indicating that the clustering of street vitality becomes less significant at broader spatial scales.

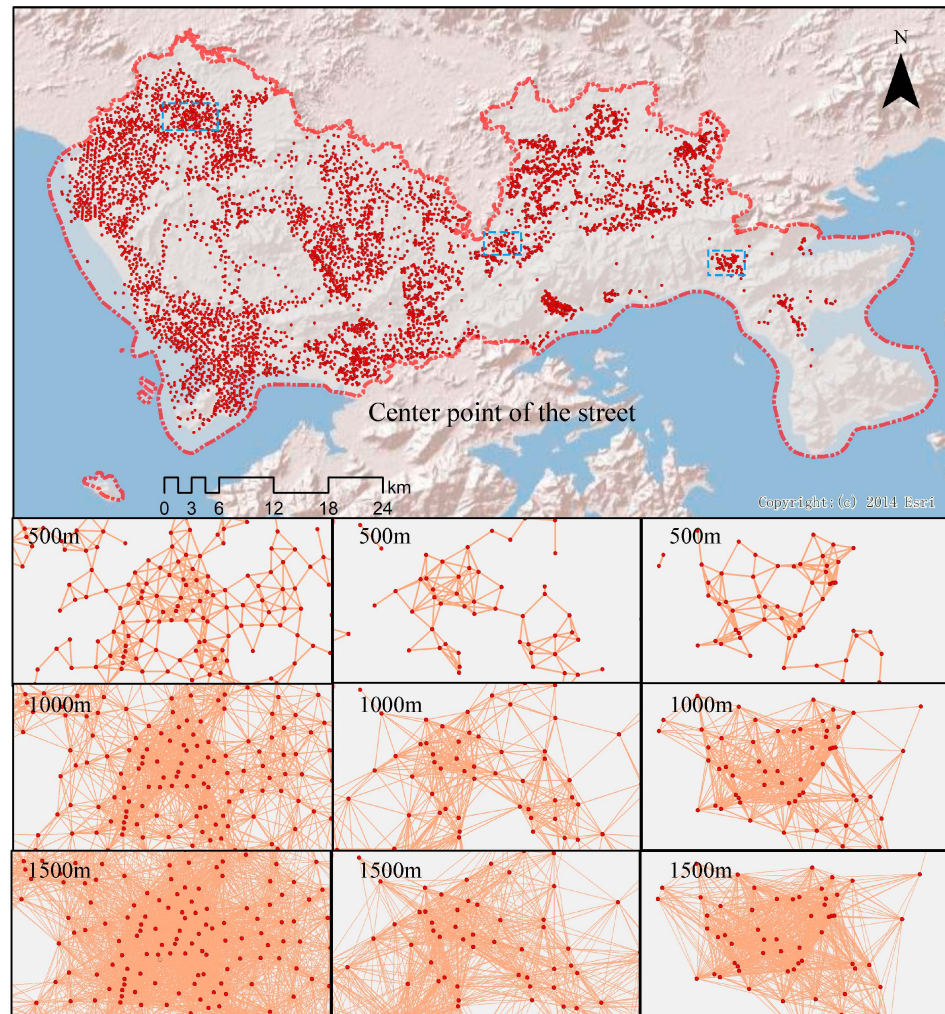


Figure 10. Street connectivity map based on the spatial weight matrix at different distances. The blue box indicates the magnified area of the figure below.

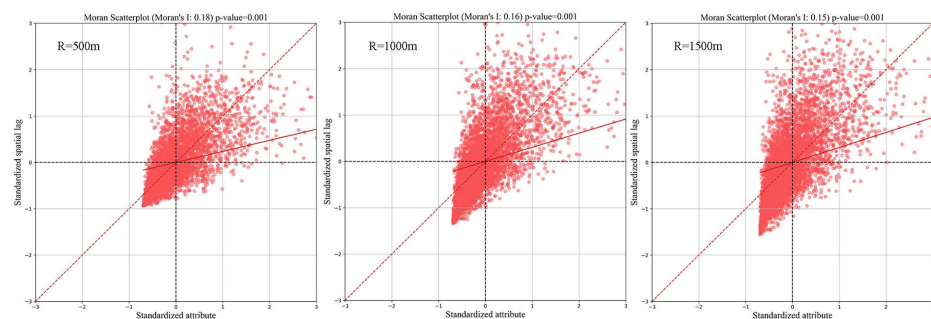


Figure 11. Moran scatterplots based on different distances.

5. Modeling Methods

Research by Li et al. has shown that the built environment has a threshold effect on street vitality [69]. The most common method to test the threshold effects of variables is the panel threshold model (PTM) proposed by Hansen [70], which can identify actual thresholds through real data simulation and statistical testing, overcoming the subjectivity

of selecting thresholds by grouped regression and cross models [71]. Based on the earlier Moran's indices, there is significant spatial correlation in street vitality. Relying solely on the PTM model and ignoring its spatial spillover effects might lead to inaccuracies in the regression results. The spatial panel Durbin model (SPDM) can control for spatial correlations among the dependent variable, explanatory variables, and error terms [72].

The built environment has both threshold effects and spatial spillover effects on street vitality, and these two effects are inseparable. Based on the strengths and weaknesses of the panel threshold model (PTM) and the spatial panel Durbin model (SPDM), and the needs of this study, referencing Wu et al.'s research [21] and adopting Feng's modeling approach [73], this paper constructs a spatial threshold model incorporating threshold and spatial effects to explore the spatial nonlinear effects of streets within different threshold ranges. Compared to PTM, it addresses several issues, such as overly high regression coefficients due to ignoring spatial spillover effects; compared to SPDM, it accounts for the widespread threshold effects in explanatory variables. Therefore, this model can better explain the mechanisms behind the formation of street vitality.

The specific steps of the computational model are as follows. First, identify the threshold effects of the built environment on street vitality through PTM. Assume there are dual thresholds λ_1 and λ_2 ($\lambda_1 < \lambda_2$) and set the dummy variable d_1 to 1 when street vitality is less than λ_1 , otherwise set it to 0; set the dummy variable d_2 to 1 when street vitality is no less than λ_1 and no greater than λ_2 , otherwise set it to 0; set the dummy variable d_3 to 1 when street vitality exceeds λ_2 , otherwise set it to 0. Subsequently, construct the interaction terms between dummy variables d_1 , d_2 , d_3 , and street vitality, to identify the sample range, and finally use the SPDM to study the impact of various control variables on street vitality under conditions constrained by different threshold variables. We define the computational method of the model as follows:

$$h_i = \gamma_0 + \rho \sum_{j=1}^n (W_{i,j} h_j) + \gamma_1 thr_i (thr_i < \lambda_1) + \gamma_2 \sum_{j=1}^n (W_{i,j} thr_j) (thr_i < \lambda_1) + \gamma_3 thr_i (\lambda_1 \leq thr_i \leq \lambda_2) + \gamma_4 \sum_{j=1}^n (W_{i,j} thr_j) (\lambda_1 \leq thr_i \leq \lambda_2) + \gamma_5 thr_i (thr_i > \lambda_2) + \gamma_6 \sum_{j=1}^n (W_{i,j} thr_j) (thr_i > \lambda_1) + \gamma_7 X_i + \varepsilon_i \quad (11)$$

$$W_{i,j} = \begin{cases} \frac{1}{d_i^2} (d_i \geq d) \\ 0 (d_i < d) \end{cases} \quad (12)$$

where γ_0 represents the expected value of h_i when all explanatory variables are 0. γ_1 , γ_3 , and γ_5 represent the estimated coefficients for the direct effects of the built environment on street vitality in the spatial threshold model, respectively. γ_2 , γ_4 , and γ_6 correspond to the estimated coefficients for the spatial spillover effects of the built environment on street vitality in the spatial threshold model, respectively. γ_7 , and γ_8 represent the coefficients for the control variable X_i and its spatial lag terms, respectively. h signifies street vitality, and i denotes the i th street. thr represents the threshold variable in the model. $W_{i,j}$ denotes the spatial connection between the i th and j th streets. X stands for the control variables. ε_i denotes the random error term. ρ is the total influence of the local street on neighboring streets. $W_{i,j}$ denotes the spatial correlation in the spatial lag model. d_i represents the distance between the centers of streets, while d_j is the planar distance calculated based on latitude and longitude. d represents the set distance thresholds, distributed as 500 m, 1000 m, and 1500 m.

6. Results

6.1. Spatial Effects of Street Vitality Using Construction Intensity as a Threshold Variable

Based on spatial weight matrices of 500 m, 1000 m, and 1500 m, we estimated the spatial autoregressive threshold model with street construction intensity as the threshold variable. The p -value for the single threshold is far below 0.01, indicating highly significant results, while the hypothesis test for the dual threshold is not statistically significant, suggesting that only one threshold exists in the development of construction intensity (Table 5). At spatial weight matrices of 500, 1000, and 1500 m, the threshold value of

construction intensity was consistently 0.1466. Based on the results of the threshold effect test, we divided construction intensity into two ranges: the segments with a construction intensity below 0.1466 are considered low-intensity, while those above this threshold are considered high-intensity.

Table 5. Test results for construction intensity as a threshold variable.

Distance Weight Matrix	Model	Threshold	F	p	Bootstrap	Crit1	Crit5	Crit10
500 m	Single threshold	0.1466 ***	117.50	0.0000	300	6.43	3.86	2.76
	Double threshold	(0.0586, 0.1466)	117.49	0.2933	300	162.46	141.53	133.97
100 m	Single threshold	0.1466 ***	126.85	0.0000	300	6.21	3.40	2.56
	Double threshold	(0.0622, 0.1466)	126.85	0.1425	300	168.32	149.42	139.86
1500 m	Single threshold	0.1466 ***	125.23	0.0000	300	6.66	3.97	2.78
	Double threshold	(0.0622, 0.1466)	125.23	0.2867	300	164.18	152.61	139.77

Note: *, **, and *** correspond to a 10%, 5%, and 1% significance level, respectively.

Based on the threshold regression model results (Table 6), it can be observed that within various spatial extents, as construction intensity increases, the spatial effects become more pronounced. In streets with high construction intensity, the construction intensity significantly and importantly affects street vitality, with the impact decreasing with increasing distance. In streets with low construction intensity, development intensity significantly influences street vitality within 500 and 1000 m, but the influence becomes insignificant at 1500 m. The impact coefficients and significance of control variables in the spatial autoregressive threshold model based on spatial weight matrices of different distances also vary.

Table 6. Spatial autoregressive threshold results under construction intensity constraints.

	Spatial Weight Matrix Based on Different Distances		
	500 m	1000 m	1500 m
Threshold	0.1466	0.1466	0.1466
Spatial autoregressive estimation coefficient			
Low range	0.0003 ***	0.0002 ***	0.0002 ***
High range	0.0006 ***	0.0003 ***	0.0003 ***
Control variables			
Functional diversity	0.0026 **	0.0027 ***	0.0022 **
Public transit facilities	1.9641 ***	1.9716 ***	1.9473 ***
Integration degree	0.4514 ***	0.4245 ***	0.2813 **
Building coverage density	5.26×10^{-7} ***	5.30×10^{-7} ***	5.28×10^{-7} ***
Public facilities and services	1.2796 ***	1.2576 ***	1.2701 ***
Sky view factor (SVF)	0.0308 ***	0.4170 **	0.4136 ***
Green view index (GVI)	-0.0178 **	-0.0200 ***	-0.0136
R ²	0.7210	0.7213	0.7209
Adjusted R ²	0.7205	0.7208	0.7204
F-statistic	1516.03	1518.53	1515.47
ROOT MSE	0.0636	0.0636	0.0636
Prob	0.0000	0.0000	0.0000
	5290	5290	5290

Note: *, **, and *** correspond to a 10%, 5%, and 1% significance level, respectively.

At a threshold of 500 m, whether for streets with low or high construction intensity, the spatial spillover effect on street vitality is significantly present, with spatial autoregression coefficients of 0.0003 and 0.006, respectively, both with *p*-values less than 0.01. Additionally, public transit accessibility and public service facilities have a significantly positive impact on street vitality. The model's explanatory power (R-squared) is 0.7205, indicating that the model can well explain the variation in the dependent variable.

At the 1000 m threshold, the positive impacts of streets with low and high construction intensities remain significant, with slight changes in the coefficients, but still shows that construction intensity significantly affects street vitality. The significance and direction

of the impact of public transportation and public service facilities are consistent with the results under the 500 m threshold.

At the 1500 m threshold, the coefficients and significance of all previously mentioned variables are similar to those at the 1000 m threshold. This suggests that despite the expanded observation range, the impacts of construction intensity, public transportation, and public service facilities on the dependent variable have not changed significantly.

For two indicators of street view images, the sky view factor (SVF) shows a significant positive impact at all spatial weighted distances (500 m, 1000 m, and 1500 m), indicating that higher SVF values are positively correlated with greater street vitality. This means that increasing the sky view factor during construction intensity constraints can enhance street vitality; the green view index (GVI) exhibits a significant negative impact at all spatial weighted distances, implying that higher GVI values are negatively correlated with lower street vitality. This suggests that increasing the green view in studies of construction intensity constraints might suppress street vitality, especially noticeable within a medium range (1000 m).

Although changes in the spatial weight thresholds resulted in variations in some coefficients within the model, the overall performance of the model (represented by the adjusted R-squared value) remained unchanged and at a high level, indicating that the model's explanatory power is similar across different spatial scales. When the spatial weight threshold changed from 500 m to 1500 m, the magnitudes of the coefficients varied, but the positive influence trend of the variables on street vitality did not change, indicating that these factors consistently impact street vitality across different spatial scales. Enhancing functional diversity, improving public transportation, increasing integration, expanding buildings' footprints, and developing public service facilities can bring positive urban effects at multiple scales. Overall, both high and low construction intensity streets have significant spatial spillover effects on street vitality at various spatial scales, which may reflect the widespread impact of construction intensity on urban spaces.

6.2. Spatial Effects of Street Vitality Using Functional Diversity as a Threshold Variable

The estimation of the spatial autoregressive threshold model used functional diversity as the threshold variable. The p -value for the single threshold is well below 0.01, indicating highly significant results. The dual-threshold hypothesis test yielded a p -value less than 0.1, significant within the 90% confidence interval. The triple-threshold test results are not statistically significant, indicating that there are two thresholds for functional diversity (Table 7). The threshold values for functional diversity within a 500 m range are 0.6832 and 2.2065; within a 1000 m range, they are 0.6832 and 1.4325; within a 1500 m range, the threshold values are 0.6832 and 1.2724.

Table 7. Results of functional diversity threshold variable test.

Distance Weight Matrix	Model	Threshold	F	p	Bootstrap	Crit1	Crit5	Crit10
500 m	Single threshold	0.6832 ***	18.58	0.0000	300	5.75	3.63	2.83
	Double threshold	(0.6832, 2.2065) *	3.07	0.0833	300	7.47	3.93	2.89
	Triple threshold	Not significant	-	-	-	-	-	-
100 m	Single threshold	0.6832 ***	31.16	0.0000	300	6.35	3.63	2.81
	Double threshold	(0.6832, 1.4325) **	4.50	0.0400	300	5.66	4.06	3.18
	Triple threshold	Not significant	-	-	-	-	-	-
1500 m	Single threshold	0.6832 ***	24.38	0.0000	300	5.79	3.52	2.94
	Double threshold	(0.6832, 1.2724) *	5.83	0.090	300	5.79	3.52	2.88
	Triple threshold	Not significant	-	-	-	-	-	-

Note: *, **, and *** correspond to a 10%, 5%, and 1% significance level, respectively.

According to the test results of the threshold effect (Table 8), taking the 500 m spatial weight matrix as an example, we have divided the construction intensity into three different ranges. When the functional diversity is below 0.6832, the street segment is considered to have low functional diversity. When the functional diversity is greater than 0.6832 but

less than 2.2065, the street segment is considered to have medium functional diversity. If the functional diversity is greater than 2.2065, the street is categorized as a high-functional diversity segment.

Table 8. Results of the spatial autoregression threshold under functional diversity constraints.

	Spatial Weight Matrix Based on Different Distances		
	500 m	1000 m	1500 m
Threshold	(0.6832, 1.2681)	(0.6832, 1.4325)	(0.6832, 1.4325)
Spatial autoregressive estimation Coefficient			
Low range	0.0004 ***	0.0002 ***	0.0002 ***
Moderate range	0.0004 ***	0.0002 ***	0.0002 ***
High range	0.0003 ***	0.0002 ***	0.0002 ***
Control variables			
Construction intensity	0.2815 ***	0.2959 ***	0.2943 ***
Public transit facilities	1.6772 ***	1.7180 ***	1.7022 ***
Integration degree	0.2997 ***	0.2921 **	0.1711 *
Building coverage density	5.06×10^{-7} ***	4.96×10^{-7} ***	4.93×10^{-7} ***
Public facilities and services	1.0531 ***	1.0578 ***	1.0726 ***
Sky view factor (SVF)	0.0719 ***	0.0808 ***	0.0785 ***
Green view index (GVI)	0.0180 **	0.0142	0.0199 **
R ²	0.7408	0.7411	0.7404
Adjusted R ²	0.7403	0.7406	0.7399
F-statistic	1508.66	1510.83	1505.05
ROOT MSE	0.0613	0.0613	0.6138
Prob	0.0000	0.0000	0.0000
Sample size	5290	5290	5290

Note: *, **, and *** correspond to a 10%, 5%, and 1% significance level, respectively.

At a spatial scale of 500 m, streets of different levels of functional diversity (high, medium, low) all have a significant positive impact on street vitality, with coefficients of 0.0004, 0.0004, and 0.0003, respectively, and all *p*-values are less than 0.01. Construction intensity, public transit accessibility, integration, building footprint, and public service facilities all show significant positive effects on the dependent variable.

At a spatial scale of 1000 m, the spatial spillover effect of functional diversity remains significantly positive. The impact of public transportation accessibility and public service facilities is similar to the 500 m model, being significantly positive. The positive effects of development intensity, public transit accessibility, and public service facilities continue to be significant.

At the 1500 m spatial scale, the spatial spillover effect of functional diversity remains significantly positive, consistent with the results from the 500 m and 1000 m models. The positive impact of functional diversity remains significant, but the coefficient decreases further, which may indicate that the influence of functional diversity weakens with increasing distance. The impacts of construction intensity, public transit accessibility, and public service facilities are consistent with previous model results.

In the context of street view images, the sky view factor (SVF) exhibits a significant positive influence at all spatial weighted distances (500 m, 1000 m, and 1500 m), with higher SVF values positively correlating with enhanced street vitality. This indicates that increasing the sky view factor can promote street vitality under functional diversity constraints, aligning with findings under construction intensity constraints. Similarly, the green view index (GVI) presents significant positive impacts at all distances, suggesting that higher GVI values are positively associated with increased street vitality. Under functional diversity constraints, the augmentation of green views may enhance street vitality, opposite to what is observed under construction intensity constraints, potentially because areas with diverse functions make better use of green spaces, fostering more interactions and activities, thereby enhancing street vitality with higher GVI values.

By comparing model results across different scales, we can see that functional diversity, construction intensity, public transit accessibility, and public service facilities have a sustained and significant spatial spillover effect on urban street vitality. Although street integration has a significant impact on street vitality at the 500 m scale, its effect diminishes

as spatial scales increase. Overall, these factors have a robust positive effect on urban street vitality across different spatial scales, although the degree of impact varies.

In urban planning practice, it is important to enhance functional diversity, optimize the public transportation network, and strengthen the construction of public service facilities to promote the integrated development of urban spaces. Additionally, strategies for street integration may need to pay more attention to the actual conditions at the local scale. Future research should consider using more detailed indices of functional diversity and exploring the impacts of different factors on broader spatial scales to reach more comprehensive conclusions.

7. Conclusions and Discussion

7.1. Conclusions

Using Shenzhen as a case study, this research utilizes multisource geographic big data and integrates PTM and SPDM models. It introduces the concept of living circles, establishes spatial weight matrices based on varying distances of living circles, and finally conducts spatial autoregressive threshold model estimations to explore the spatial nonlinear effects of street vitality under different thresholds of construction intensity and functional diversity. The study results confirm that under the constraints of construction intensity and functional diversity, street vitality exhibits significant spatial nonlinear effects, which conform to the distance decay mechanism. The study also finds that there is one threshold for construction intensity, while functional diversity has two thresholds. Furthermore, we found that both construction intensity and functional diversity have significant positive impacts on street vitality across different distance weight ranges, but these impacts are subject to threshold effects.

This means that enhancing the construction intensity and functional diversity of a particular street not only boosts its own vitality but also positively affects the vitality of surrounding streets, thereby promoting the overall vitality of the city. At the same time, the threshold effects of construction intensity and functional diversity reveal nonlinear changes in street vitality, as these factors vary. This means that within a certain range, enhancing construction intensity and functional diversity can significantly boost street vitality, but once a certain threshold is exceeded, the positive effects will diminish.

Within various distance weight ranges, the density of public transportation services has the greatest impact on street vitality in Shenzhen, followed by the density of public facility services. Urban integration, which ranks third in importance, along with public transportation services, are indicators of street accessibility. This indicates that for a densely populated, first-tier international metropolis, like Shenzhen, there is a massive residential and commuting population. The effectiveness of public transportation services directly affects the daily travel efficiency and quality of life of urban residents. Moreover, a good public transportation system can reduce traffic congestion and increase energy efficiency. Additionally, high-quality public facilities and transportation services can elevate the living standards of all residents and reduce social inequality. Therefore, for a major first-tier city, like Shenzhen, investing in and developing an efficient public transportation system and comprehensive public facilities is a key strategy for achieving socio-economic development, enhancing urban competitiveness, and improving the quality of life for residents.

For street view characteristics at the human scale, when construction intensity is used as the threshold variable, the spatial autoregressive coefficient of the green view index is negative, which is consistent with Jiang's findings. Although streets with high green view index values signify higher quality streets, this does not necessarily mean higher pedestrian flow and vitality, requiring more research to confirm this conclusion [74].

7.2. Discussion

In the field of economics, many scholars have found through spatial econometric models that urbanization has a significant spatial spillover effect on local energy efficiency. At the same time, many scholars have used threshold models to explore the nonlinear

relationship between urbanization and local energy efficiency. However, while a lot of research has explored the complex relationships of the built environment in the formation of street vitality, few have investigated the spatial effects of street vitality, and even fewer have examined the nonlinear effects of the built environment on street vitality in conjunction with spatial effects. This study focuses on how street vitality and its spatial effects vary when street construction intensity and functional diversity are within different ranges, and it sets spatial weight matrices at various distances. The results confirm the presence of significant spatial nonlinear effects on street vitality, which can help us better understand the mechanisms behind the formation of street vitality.

However, there are still some areas in the article that merit further consideration. Firstly, although the LBS data based on Baidu Huiyan include hundreds of millions of passive samples, they still cannot fully represent the specific distribution of the street population, such as users without Baidu apps on their phones, users who have not authorized location permissions, and some who do not use mobile phones at all. Secondly, the data we obtained have been coarsened; even though we processed the data with ArcGIS Pro to obtain as accurate information as possible, discrepancies still occurred. Thirdly, since the process of street vitality formation is extremely complex, our selected control variables cannot fully explain street vitality; moreover, although we used different buffer distances for different types of streets, real-world streets are complex and interlocking, and even main roads have significant differences. This study also raises some issues that need further discussion. Firstly, since the basis of spatial analysis is the setting of scales, when the research scale differs, the research results often vary. This study only sets three different distance thresholds. If we further reduce the interval between thresholds and increase the number of distance thresholds, will it yield more detailed results? Secondly, this study only conducted empirical research on Shenzhen, and whether similar spatial effects occur in different types of cities and regional contexts needs further verification. Finally, spatial effects including spatial agglomeration effects, spatial spillover effects, spatial heterogeneity, and spatial scale effects, etc., need further in-depth exploration.

Overall, the method proposed in this paper represents a proactive attempt to explore the spatial effects of street vitality and the nonlinear effects of the built environment on street vitality, providing a theoretical foundation for further understanding the mechanisms of street vitality formation, and offering nuanced suggestions for urban street management and construction.

Author Contributions: Conceptualization, Jilong Li; Methodology, Jilong Li and Shiping Lin; Software, Jilong Li, Jie Zeng and Jiacheng Chen; Validation, Jilong Li; Formal analysis, Jilong Li and Jiacheng Chen; Investigation, Jilong Li, Niuniu Kong and Jie Zeng; Resources, Jilong Li and Yilin Ke; Data curation, Jilong Li and Yilin Ke; Writing—original draft, Jilong Li; Writing—review & editing, Shiping Lin; Visualization, Niuniu Kong, Yilin Ke, Jie Zeng and Jiacheng Chen; Supervision, Niuniu Kong, Shiping Lin and Jiacheng Chen; Project administration, Jilong Li and Shiping Lin; Funding acquisition, Jilong Li and Shiping Lin. All authors have read and agreed to the published version of the manuscript.

Funding: This research was funded by the National Natural Science Foundation of China, grant number “52268011” (First Fund) and the 2023 Hainan Province Graduate Student Innovation Research Project, ID Qhys2023-208.

Data Availability Statement: The authors have not obtained permission to publish the data. Therefore, the data can be obtained from the corresponding author upon reasonable request.

Acknowledgments: We appreciate the support provided by Hainan University.

Conflicts of Interest: The authors declare no conflicts of interest. The funding sponsors had no role in the design of the study; in the collection, analysis, or interpretation of data; in the writing of the manuscript; or in the decision to publish results.

References

- Jacobs, J. *The Death and Life of Great American Cities*; Vintage Books, a Division of Random House: New York, NY, USA, 1961; 240p.
- Wangbao, L. Spatial impact of the built environment on street vitality: A case study of the Tianhe District, Guangzhou. *Front. Environ. Sci.* **2022**, *10*, 966562. [[CrossRef](#)]
- Hass-Klau, C. *The Pedestrian and City Traffic*; Belhaven Press: London, UK, 1990; 277p.
- Fan, Z.; Su, T.; Sun, M.; Noyman, A.; Zhang, F.; Pentland, A.S.; Moro, E. Diversity beyond density: Experienced social mixing of urban streets. *PNAS Nexus* **2023**, *2*, pgad077. [[CrossRef](#)]
- Wang, S.; Deng, Q.; Jin, S.; Wang, G. Re-Examining Urban Vitality through Jane Jacobs' Criteria Using GIS-sDNA: The Case of Qingdao, China. *Buildings* **2022**, *12*, 1586. [[CrossRef](#)]
- Li, M.; Pan, J. Assessment of Influence Mechanisms of Built Environment on Street Vitality Using Multisource Spatial Data: A Case Study in Qingdao, China. *Sustainability* **2023**, *15*, 1518. [[CrossRef](#)]
- Wu, W.; Ma, Z.; Guo, J.; Niu, X.; Zhao, K. Evaluating the Effects of Built Environment on Street Vitality at the City Level: An Empirical Research Based on Spatial Panel Durbin Model. *Int. J. Environ. Res. Public Health* **2022**, *19*, 1664. [[CrossRef](#)] [[PubMed](#)]
- Hu, X.; Shen, X.; Shi, Y.; Li, C.; Zhu, W. Multidimensional Spatial Vitality Automated Monitoring Method for Public Open Spaces Based on Computer Vision Technology: Case Study of Nanjing's Daxing Palace Square. *ISPRS Int. J. Geo-Inf.* **2024**, *13*, 48. [[CrossRef](#)]
- Wang, H.; Tang, J.; Xu, P.; Chen, R.; Yao, H. Research on the Influence Mechanism of Street Vitality in Mountainous Cities Based on a Bayesian Network: A Case Study of the Main Urban Area of Chongqing. *Land* **2022**, *11*, 728. [[CrossRef](#)]
- Li, X.; Qian, Y.; Zeng, J.; Wei, X.; Guang, X. The Influence of Strip-City Street Network Structure on Spatial Vitality: Case Studies in Lanzhou, China. *Land* **2021**, *10*, 1107. [[CrossRef](#)]
- Guimarães, P.; Figueiredo, O.; Woodward, D. Accounting for Neighboring Effects in Measures of Spatial Concentration. *J. Reg. Sci.* **2011**, *51*, 678–693. [[CrossRef](#)]
- Lychagin, S.; Pinkse, J.; Slade, M.E.; Van Reenen, J. Spillovers in Space: Does Geography Matter? *J. Ind. Econ.* **2016**, *64*, 295–335. [[CrossRef](#)]
- Zhou, R.; Zhang, Y.; Gao, X. The Spatial Interaction Effect of Environmental Regulation on Urban Innovation Capacity: Empirical Evidence from China. *Int. J. Environ. Res. Public Health* **2021**, *18*, 4470. [[CrossRef](#)] [[PubMed](#)]
- Petrović, A.; van Ham, M.; Manley, D. Where Do Neighborhood Effects End? Moving to Multiscale Spatial Contextual Effects. *Ann. Am. Assoc. Geogr.* **2022**, *112*, 581–601. [[CrossRef](#)]
- Zhu, J.G.; Li, X.J. The Impact Effects of Industrial Agglomeration on the High-Quality Growth of Regional Economy—A Perspective Based on Spatial Spillover Effects. *Econ. Geogr.* **2022**, *42*, 1–9.
- Heng, Y.; Zhang, F. The complete path effect model of the three-dimensional street environment on street usage time. *J. Urban Des.* **2021**, *26*, 514–529. [[CrossRef](#)]
- Yue, H.; Zhu, X. Exploring the Relationship between Urban Vitality and Street Centrality Based on Social Network Review Data in Wuhan, China. *Sustainability* **2019**, *11*, 4356. [[CrossRef](#)]
- Zhang, S.; Zhu, D.; Yao, X.; Cheng, X.; He, H.; Liu, Y. The Scale Effect on Spatial Interaction Patterns: An Empirical Study Using Taxi O-D data of Beijing and Shanghai. *IEEE Access* **2018**, *6*, 51994–52003. [[CrossRef](#)]
- Liu, C.; Lu, J.; Fu, W.; Zhou, Z. Second-hand housing batch evaluation model of zhengzhou city based on big data and MGWR model. *J. Intell. Fuzzy Syst.* **2022**, *42*, 4221–4240. [[CrossRef](#)]
- Tu, J. Spatially varying relationships between land use and water quality across an urbanization gradient explored by geographically weighted regression. *Appl. Geogr.* **2011**, *31*, 376–392. [[CrossRef](#)]
- Wu, W.; Dang, Y.; Zhao, K.; Chen, Z.; Niu, X. Spatial nonlinear effects of urban vitality under the constraints of development intensity and functional diversity. *Alex. Eng. J.* **2023**, *77*, 645–656. [[CrossRef](#)]
- Vidal Domper, N.; Hoyos-Bucheli, G.; Benages Albert, M. Jane Jacobs's Criteria for Urban Vitality: A Geospatial Analysis of Morphological Conditions in Quito, Ecuador. *Sustainability* **2023**, *15*, 8597. [[CrossRef](#)]
- Liu, M.; Jiang, Y.; He, J. Quantitative Evaluation on Street Vitality: A Case Study of Zhoujiadu Community in Shanghai. *Sustainability* **2021**, *13*, 3027. [[CrossRef](#)]
- Pan, J.; Zhu, X.; Zhang, X. Urban Vitality Measurement and Influence Mechanism Detection in China. *Int. J. Environ. Res. Public Health* **2023**, *20*, 46. [[CrossRef](#)] [[PubMed](#)]
- Han, Y.; Ye, Y.; Qin, C. Nonlinear relationship between the urban form and street vitality: A data informed approach involving twelve Chinese cities. In *Annual Conference Proceedings of the XXVIII International Seminar on Urban Form*; University of Strathclyde Publishing: Glasgow, UK, 2022; pp. 371–380. ISBN 9781914241161.
- Xu, J.; Xiong, Q.; Jing, Y.; Xing, L.; An, R.; Tong, Z.; Liu, Y.; Liu, Y. Understanding the nonlinear effects of the street canyon characteristics on human perceptions with street view images. *Ecol. Indic.* **2023**, *154*, 110756. [[CrossRef](#)]
- Li, Y.; Yabuki, N.; Fukuda, T. Exploring the association between street built environment and street vitality using deep learning methods. *Sustain. Cities Soc.* **2022**, *79*, 103656. [[CrossRef](#)]
- Zhao, K.; Guo, J.; Ma, Z.; Wu, W. Exploring the Spatiotemporal Heterogeneity and Stationarity in the Relationship between Street Vitality and Built Environment. *Sage Open* **2023**, *13*, 21582440231152226. [[CrossRef](#)]
- Fan, Z.; Pei, T.; Ma, T.; Du, Y.; Song, C.; Liu, Z.; Zhou, C. Estimation of urban crowd flux based on mobile phone location data: A case study of Beijing, China. *Comput. Environ. Urban Syst.* **2018**, *69*, 114–123. [[CrossRef](#)]

30. Chen, Z.; Gong, Z.; Yang, S.; Ma, Q.; Kan, C. Impact of extreme weather events on urban human flow: A perspective from location-based service data. *Comput. Environ. Urban Syst.* **2020**, *83*, 101520. [[CrossRef](#)]
31. Martí, P.; Serrano-Estrada, L.; Nolasco-Cirugeda, A. Social Media data: Challenges, opportunities and limitations in urban studies. *Comput. Environ. Urban Syst.* **2019**, *74*, 161–174. [[CrossRef](#)]
32. Wu, W.; Niu, X. Influence of Built Environment on Urban Vitality: Case Study of Shanghai Using Mobile Phone Location Data. *J. Urban Plan. Dev.* **2019**, *145*, 04019007. [[CrossRef](#)]
33. Yue, Y.; Zhuang, Y.; Yeh, A.G.; Xie, J.Y.; Ma, C.L.; Li, Q.Q. Measurements of POI-based mixed use and their relationships with neighbourhood vibrancy. *Int. J. Geogr. Inf. Sci.* **2017**, *31*, 658–675. [[CrossRef](#)]
34. Huang, H.; Gartner, G.; Krisp, J.M.; Raubal, M.; Van De Weghe, N. Location based services: Ongoing evolution and research agenda. *J. Locat. Based Serv.* **2018**, *12*, 63–93. [[CrossRef](#)]
35. Yu, S.S. Urban Road Landscape Research Based on a Multivariate Perspective. Ph.D. Thesis, Nanjing Forestry University, Nanjing, China, 2023. [[CrossRef](#)]
36. Gehl, J. *Life between Buildings: Using Public Space*; Van Nostrand Reinhold: New York, NY, USA, 1987; 202p.
37. Montgomery, J. Making a city: Urbanity, vitality and urban design. *J. Urban Des.* **1998**, *3*, 93–116. [[CrossRef](#)]
38. Zhou, H.; He, S.; Cai, Y.; Wang, M.; Su, S. Social inequalities in neighborhood visual walkability: Using Street View imagery and deep learning technologies to facilitate healthy city planning. *Sustain. Cities Soc.* **2019**, *50*, 101605. [[CrossRef](#)]
39. Shen, Y.; Karimi, K. Urban function connectivity: Characterisation of functional urban streets with social media check-in data. *Cities* **2016**, *55*, 9–21. [[CrossRef](#)]
40. Sulis, P.; Manley, E.; Zhong, C.; Batty, M. Using mobility data as proxy for measuring urban vitality. *J. Spat. Inf. Sci.* **2018**, *2018*, 137–162. [[CrossRef](#)]
41. Liu, S.; Zhang, L.; Long, Y.; Long, Y.; Xu, M. A New Urban Vitality Analysis and Evaluation Framework Based on Human Activity Modeling Using Multi-Source Big Data. *ISPRS Int. J. Geo-Inf.* **2020**, *9*, 617. [[CrossRef](#)]
42. Xia, C.; Yeh, A.G.; Zhang, A. Analyzing spatial relationships between urban land use intensity and urban vitality at street block level: A case study of five Chinese megacities. *Landsc. Urban Plan.* **2020**, *193*, 103669. [[CrossRef](#)]
43. Kim, Y. Seoul's Wi-Fi hotspots: Wi-Fi access points as an indicator of urban vitality. *Comput. Environ. Urban Syst.* **2018**, *72*, 13–24. [[CrossRef](#)]
44. Liu, X.; Tian, Y.; Zhang, X.; Wan, Z. Identification of Urban Functional Regions in Chengdu Based on Taxi Trajectory Time Series Data. *ISPRS Int. J. Geo-Inf.* **2020**, *9*, 158. [[CrossRef](#)]
45. Zeng, P.; Wei, M.; Liu, X. Investigating the Spatiotemporal Dynamics of Urban Vitality Using Bicycle-Sharing Data. *Sustainability* **2020**, *12*, 1714. [[CrossRef](#)]
46. Sun, M.; Fan, H. Detecting and Analyzing Urban Centers Based on the Localized Contour Tree Method Using Taxi Trajectory Data: A Case Study of Shanghai. *ISPRS Int. J. Geo-Inf.* **2021**, *10*, 220. [[CrossRef](#)]
47. Cervero, R.; Bernick, M. *Transit Villages in the 21st Century*; McGraw-Hill: New York, NY, USA, 1997; 387p.
48. Chen, L.; Zhao, L.; Xiao, Y.; Lu, Y. Investigating the spatiotemporal pattern between the built environment and urban vibrancy using big data in Shenzhen, China. *Comput. Environ. Urban Syst.* **2022**, *95*, 101827. [[CrossRef](#)]
49. Ye, Y.; Li, D.; Liu, X. How block density and typology affect urban vitality: An exploratory analysis in Shenzhen, China. *Urban Geogr.* **2017**, *39*, 631–652. [[CrossRef](#)]
50. Li, Q.; Cui, C.; Liu, F.; Wu, Q.; Run, Y.; Han, Z. Multidimensional Urban Vitality on Streets: Spatial Patterns and Influence Factor Identification Using Multisource Urban Data. *ISPRS Int. J. Geo-Inf.* **2022**, *11*, 2. [[CrossRef](#)]
51. Lu, S.; Shi, C.; Yang, X. Impacts of Built Environment on Urban Vitality: Regression Analyses of Beijing and Chengdu, China. *Int. J. Environ. Res. Public Health* **2019**, *16*, 4592. [[CrossRef](#)]
52. Baskin, C.W.; Christaller, W. *Central Places in Southern Germany*; Prentice-Hall: Englewood Cliffs, NJ, USA, 1966; 230p.
53. Fu, W.; Luo, C.; He, S. Does Urban Agglomeration Promote the Development of Cities? An Empirical Analysis Based on Spatial Econometrics. *Sustainability* **2022**, *14*, 14512. [[CrossRef](#)]
54. Xiang, Y.; Zhang, T.; Ren, Q. The Spatial Spillover Effects of Infrastructure on Economic Growth in Shenyang Economic Zone. *Front. Eng. Manag.* **2016**, *3*, 290. [[CrossRef](#)]
55. Hu, C.; Liu, W.; Jia, Y.; Jin, Y. Characterization of Territorial Spatial Agglomeration Based on POI Data: A Case Study of Ningbo City, China. *Sustainability* **2019**, *11*, 5083. [[CrossRef](#)]
56. Lynch, K. *The Image of the City*; Technology Press: Cambridge, MA, USA, 1960; 194p.
57. Artmann, M.; Kohler, M.; Meinel, G.; Gan, J.; Joja, I.-C. How smart growth and green infrastructure can mutually support each other—A conceptual framework for compact and green cities. *Ecol. Indic.* **2019**, *96*, 10–22. [[CrossRef](#)]
58. Kim, L.; Moon, T. The Effect of Compact City's Spatial Factors on Social Sustainability. *Hous. Stud.* **2010**, *18*, 51–72.
59. Ma, Z. Deep exploration of street view features for identifying urban vitality: A case study of Qingdao city. *Int. J. Appl. Earth Obs. Geoinf.* **2023**, *123*, 103476. [[CrossRef](#)]
60. Wang, M.; Pei, X.; Zhang, M.; Tang, Y. Evaluation and Optimization of Urban Public Space Accessibility for Residents' Satisfaction: A Case Study of Nanshan District, Shenzhen City. *Buildings* **2023**, *13*, 2624. [[CrossRef](#)]
61. Chen, S.; Biljecki, F. Automatic assessment of public open spaces using street view imagery. *Cities* **2023**, *137*, 104329. [[CrossRef](#)]
62. Xiao, Z.P.; Chai, Y.W.; Zhang, Y. Review of Progress in Domestic and International Living Circle Planning Research and Planning Practice. *Planner* **2014**, *30*, 89–95.

63. Moreno, C.; Allam, Z.; Chabaud, D.; Gall, C.; Pratlong, F. Introducing the “15-Minute City”: Sustainability, Resilience and Place Identity in Future Post-Pandemic Cities. *Smart Cities* **2021**, *4*, 93–111. [[CrossRef](#)]
64. Manifesty, O.R.; Park, J.Y. A Case Study of a 15-Minute City Concept in Singapore’s 2040 Land Transport Master Plan: 20-Minute Towns and a 45-Minute City. *Int. J. Sustain. Transp. Technol.* **2022**, *5*, 1–11. [[CrossRef](#)]
65. Guan, Y.B.; Ma, R.; Kong, Y.F. Research on the Location Model of Urban Community Convenience Service Centers. *J. Geo-Inf. Sci.* **2023**, *25*, 2164–2177.
66. Xiao, Z.P.; Han, L.W.; Chai, Y.W. Considerations on Integrating Living Circle Planning into National Spatial Planning. *Planner* **2022**, *38*, 145–151.
67. Ryus, P.; Musunuru, A.; Bonneson, J.; Kothuri, S.; Monsere, C.; McNeil, N.; LaJeunesse, S.; Nordback, K.; Kumfer, W.; Currin, S.; et al. *Guide to Pedestrian Analysis*; The National Academies Press: Washington, DC, USA, 2022.
68. Zhang, H.L.; Ge, P. Analysis of the Relationship between the Proportion of Elderly Pedestrians at Signalized Intersections and Pedestrian Walking Speed. *Sci. Technol. Eng.* **2018**, *18*, 287–292.
69. Li, J.; Lin, S.; Kong, N.; Ke, Y.; Zeng, J.; Chen, J. Nonlinear and Synergistic Effects of Built Environment Indicators on Street Vitality: A Case Study of Humid and Hot Urban Cities. *Sustainability* **2024**, *16*, 1731. [[CrossRef](#)]
70. Hansen, B.E. Threshold effects in non-dynamic panels: Estimation, testing, and inference. *J. Econom.* **1999**, *93*, 345–368. [[CrossRef](#)]
71. Yang, Q.; Song, D. How does environmental regulation break the resource curse: Theoretical and empirical study on China. *Resour. Policy* **2019**, *64*, 101480. [[CrossRef](#)]
72. Elhorst, J.P. *Spatial Econometrics: From Cross-Sectional Data to Spatial Panels*, 1st ed.; Springer: Berlin/Heidelberg, Germany, 2014.
73. Feng, Y.; Liu, Y.; Yuan, H. The spatial threshold effect and its regional boundary of new-type urbanization on energy efficiency. *Energy Policy* **2022**, *164*, 112866. [[CrossRef](#)]
74. Jiang, Y.; Han, Y.; Liu, M.; Ye, Y. Street vitality and built environment features: A data-informed approach from fourteen Chinese cities. *Sustain. Cities Soc.* **2022**, *79*, 103724. [[CrossRef](#)]

Disclaimer/Publisher’s Note: The statements, opinions and data contained in all publications are solely those of the individual author(s) and contributor(s) and not of MDPI and/or the editor(s). MDPI and/or the editor(s) disclaim responsibility for any injury to people or property resulting from any ideas, methods, instructions or products referred to in the content.